ELECTROMOTION 2001
June 19-20, 2001
Bologna - ITALY

NEW DESIGN OF A SOFT MAGNETIC COMPOSITE TRANSVERSE FLUX MACHINE WITH SPECIAL ATTENTION ON THE LOSS MECHANISMS

R. Blissenbach, G. Henneberger

Department of Electrical Machines (IEM)
Aachen Institute of Technology (RWTH)
Germany

Abstract - The development of a new design of a transverse flux machine with soft magnetic composite will be described in this paper. The optimization of the magnetic circuit by means of 3D-FEM, the identification and calculation of the losses, partly with a 3D solver with time stepping procedure and the effects of a suitable current excitation on the efficiency and operating range wili be presented.

I. INTRODUCTION

Transverse flux motors have an excellent torque-to-volume ratio in comparison with conventional machines. The reason for the high specific torque is the decoupling of magnetic flux paths and armature coils, which permits a very high current loading and consequently a high force density by simply enlarging the number of pole pairs. For this reason, the transverse flux machine is especially suited for direct drive applications in electric vehicles and railways.
Special attention has to be paid to the investigation of the loss mechanisms both in the active parts and the carrier and housing regions because this is very important for the prediction of the machine performance.

II. THE MACHINE LAYOUT

The geometry of the three phase magnetic circuit for a double pole pitch in circumference direction is presented in Fig. 1. The armature winding in the inner stator is surrounded by the stator poles made of a soft magnetic composite.
The stator poles are arranged circumferentially in a distance of a double pole pitch. The two pole shoes of one stator pole are shifted against each other with an electrical angle of 180°, which is equivalent to a pole pitch.
In the external rotor a flux concentrating design with soft magnetic composite pieces between the rare earth permanent magnets, which are magnetized with alternating polarity in circumference direction, is applied.
A detailed description of the mechanical layout of a transverse flux machine, whose basic structure is similar to that of the machine presented here, can be found in [1] and [2].

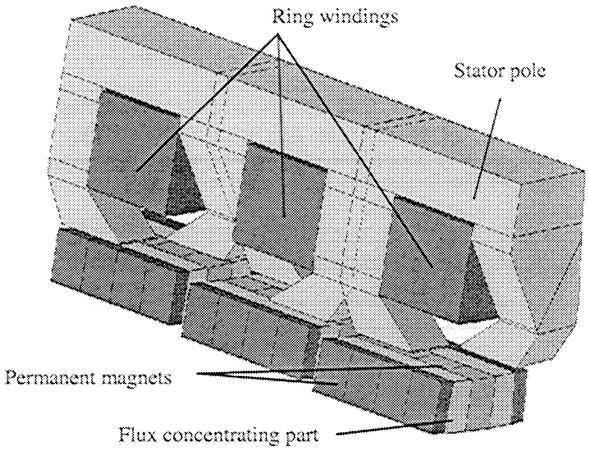

Fig. 1. View of a double pole pitch of the magnetic circuit

III. OPTIMIZATION OF THE MAGNETIC CIRCUIT

3D-FEM calculations were used to optimize the geometry of the magnetic circuit. Fig. 2 shows the distribution of the flux density in a linearized model for the smallest symmetry unit of the machine. Because of the high number of poles the calculation of a linearized model is sufficient.
It is a characteristic of the transverse flux machine that many of the design parameters, as shown in Fig. 2, are independent of each other and can be chosen arbitrarily. A huge number of parameter variations finally lead to an optimized design.
Main target function in the optimization process is a maximum output torque with a minimum torque ripple in consideration of the limits for phase voltage and current given by the inverter.

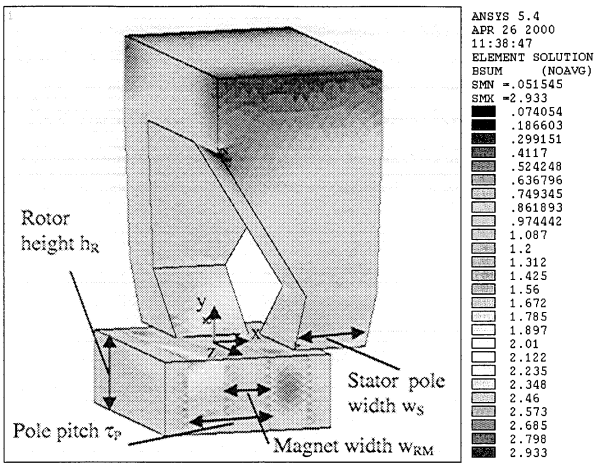

Fig. 2. Flux density distribution with design parameters

Fixed parameters in the optimization process are the machine diameter (D = 315mm) and the maximum speed (n_{max} = 1200rpm), both given by the specifications for the application as a wheel hub motor in an electric vehicle.
Another specification for the operating range is that the maximum torque should be available at half the maximum speed without reaching the maximum inverter voltage. As the stator phase voltage is strongly influenced by the number of poles and number of stator winding turns, these parameters have to be investigated.
With a smaller number of winding turns the current exceeds the limit of the maximum inverter current if the same torque should be reached, whereas with a higher number of winding turns the phase voltage exceeds the limited inverter voltage. In Fig. 3 the dependency of the phase voltage and the output torque at 600 rpm on the number of poles with a constant number of winding turns (w = 16) is depicted. The dashed line shows the limited inverter voltage of 220V. Because of the fixed diameter the variation of the number of poles is equivalent to the variation of the pole pitch.
In consideration of a necessary safety margin the number of poles should be below 43 poles although this is not the optimal number of poles for the torque.

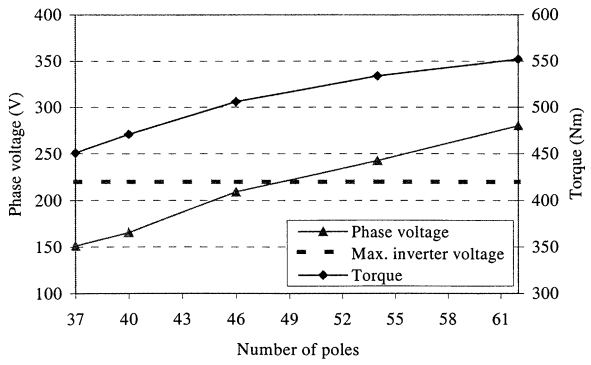

Fig. 3. Influence of stator pole number on torque and voltage

The variations of the other design parameters with their influence on the output torque and torque ripple are shown in the following diagrams. It is obvious that both target functions, maximum torque and minimum torque ripple, together can only be fulfilled to a certain degree.
Fig. 4 shows an explicit optimum for the magnet width with regard to a maximum torque.
Fig. 5 displays the big effect of the stator pole width on the torque ripple whereas the modification of the output torque is quite small.
At last Fig. 6 shows that for a further increase of approximately 4% for the output torque, an increase of 30 % in permanent magnet volume (rotor height rises from 10 to 13mm) is needed.

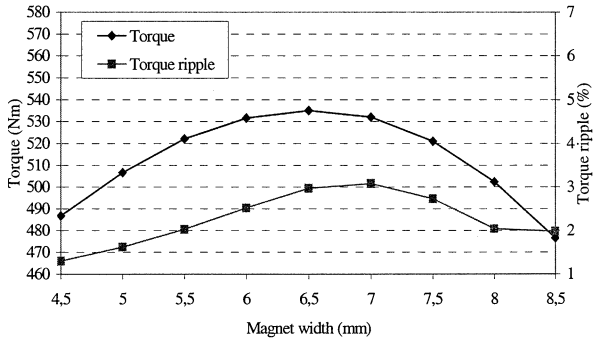

Fig. 4. Variation of magnet width

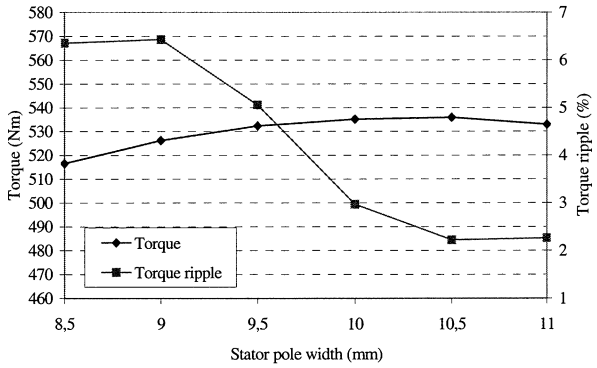

Fig. 5. Variation of stator pole width

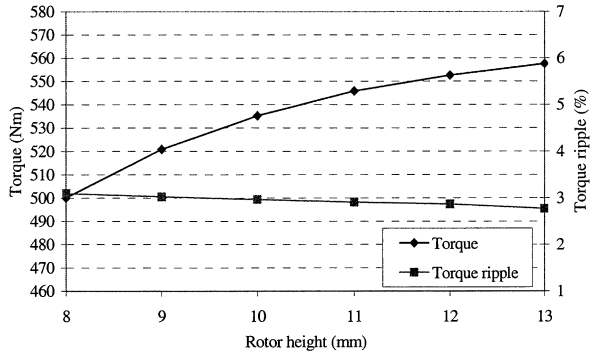

Fig. 6. Variation of rotor pole height

The torque curves for the three phases and their superposition to the total torque are shown in Fig. 7 for the optimized design.
With a r.m.s. phase current of 90A an output torque of 530Nm with a torque ripple of 3 % is obtained.
The dependency of the output torque and the power factor on the stator current is depicted in Fig. 8. Because of fringing effects the leakage inductance is big and causes an inductive voltage drop. This is a characteristic of the transverse flux machine presented here and leads to a poor power factor at high load.
The shape of the torque curve points out that with higher currents even higher torque values are reachable.
The final machine design consists of 40 poles and an outer diameter of the active parts of 315mm and an axial length of 115mm.
The air-gap length was chosen to 0.8mm. The active mass is about 30kg, including the permanent magnets and copper windings.
With the values mentioned above a torque per unit active mass of 17.9Nm/kg and a torque per unit active volume of 58.6kNm/m^3 is resulting.

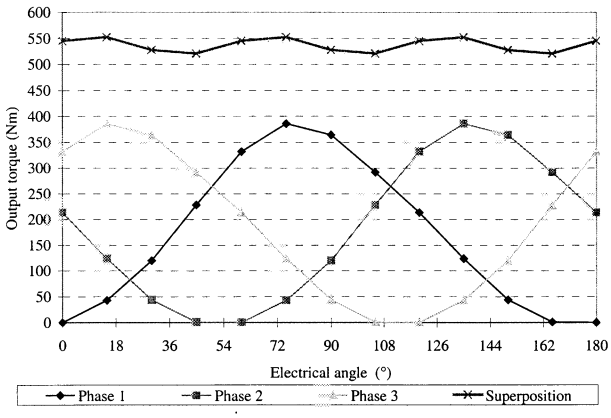

Fig. 7. Three phase superposition of the torque

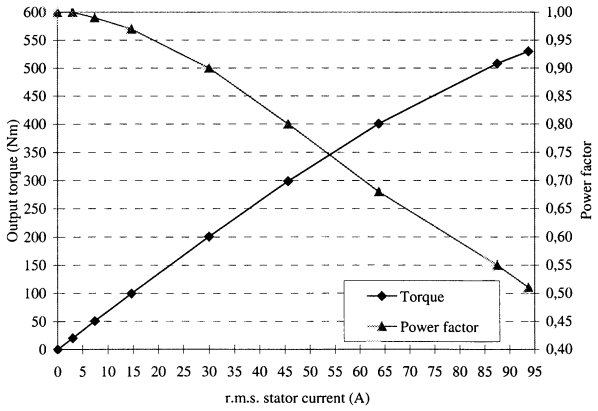

Fig. 8. Output torque and power factor versus stator current

IV. CALCULATION OF THE MACHINE LOSSES

In the first section the complete arrangement of the active machine parts have been shown. Carriers with suitable geometry and material have to be chosen for both stator and rotor in order to mount the active parts. In case of conducting carrier regions the investigation of eddy current losses in these parts is very important for the prediction of the machine performance. To prevent the risk of demagnetization of the NdFeB magnets at high temperature, which have a good electric conductivity, the eddy currents in the magnets also have to be examined. Besides these additional losses, iron losses in the magnetic flux guiding regions and copper losses in the winding also occur.
These different loss mechanisms will be examined separately in the following.

A. Copper losses

The calculation of the ohmic losses in the winding can be done with the DC resistance because HF litz is used to avoid current displacement. The thermal behavior of the DC resistance is given by the equation:

$$R' = R(\vartheta) = R_{20} \cdot (1 + \alpha_{20} \cdot (\Delta\vartheta)) \quad (1)$$

With the phase resistance R_{20}=21mΩ and the temperature coefficient $\alpha_{20} = 0{,}00393\frac{1}{K}$ for 20°C the total copper losses result to:

$$P_{Cu} = 3 \cdot I^2 \cdot R' \quad (2)$$

B. Iron losses in the soft magnetic composite

The complete stator poles and the flux concentrating parts in the rotor are made of a soft magnetic composite (Somaloy 500). Detailed information about the properties of such materials can be found in [3] and [4]. This material tends to have very low eddy current losses because the conduction between grains is very small. Therefore, the iron losses mainly consist of hysteresis losses and for different frequencies the specific iron losses in a soft magnetic composite can be assumed to rise linear with the frequency:

$$p_{Fe} \sim f \quad (3)$$

The measured influence of the flux density on the specific iron losses for a fixed frequency of 50Hz is shown in Fig. 9. The result of the interpolation curve is a function of the following type:

$$p_{Fe} \sim B^{1.7} \quad (4)$$

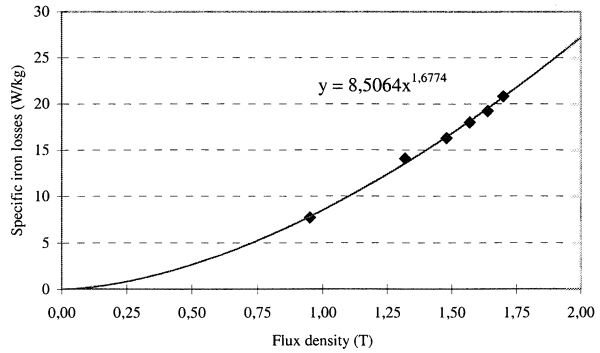

Fig. 9. Specific iron losses versus flux density for 50Hz

The dependence of the specific iron losses on frequency and flux density in (3) and (4) coincides quite well with the specific loss values given in data sheets by the manufacturer.

The next step is the calculation of the distribution of flux density for several regions in the machine geometry from static FE-results. For two regions the flux density components with respect to the rotor position are shown in Fig. 10 and Fig. 11. In the stator core back the predominant flux density component is in axial direction (B_z) and it mainly consists of the fundamental component of the frequency.

In the pole shoe of the stator core all flux density components contribute to the iron losses with especially the circumferential component (B_x) showing higher harmonics of the frequency.

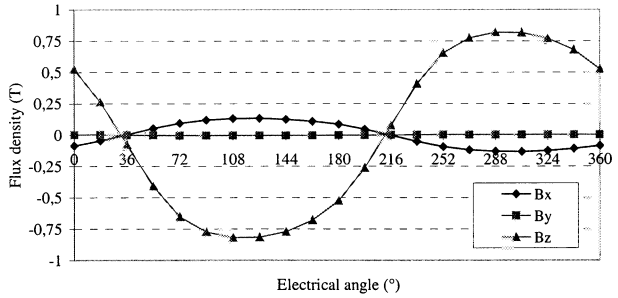

Fig. 10. Flux density components in the stator core back

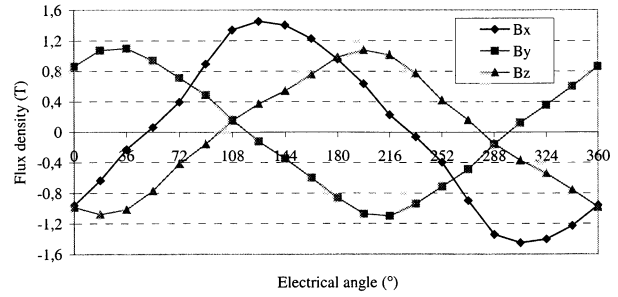

Fig. 11. Flux density components in the pole shoes

The appearance of all flux density components in the pole shoes points out the advantages of the soft magnetic composite over laminated steel for this application. With laminated steel high eddy current losses caused by alternating fields perpendicular to the direction of lamination would be produced.

After a fourier analysis the calculation of the iron losses is done for every harmonic with dependence on the frequency and flux density in the several regions.

A superposition yields the total iron loss of the machine with m_i being the mass of the actual iron region:

$$P_{Fe} = \sum_i p_{Fe}\left(\hat{B}_i, f\right) \cdot m_i \qquad (5)$$

C. Eddy current losses in permanent magnets and carrier regions

The static flux in the rotor caused by the permanent magnets is modulated by the geometry of the stator when the machine is turning and fed with a stator current. This induces eddy currents in all electrical conducting regions of the rotor.

In contrast to the soft magnetic composite of the flux concentrating parts the NdFeB permanent magnets have a quite good electric conductivity.

Another important point concerning eddy currents is the selection of the carrier and housing materials for mounting the active parts in the rotor, because leakage field components are expected in these regions. Therefore, the fixation of the active rotor parts has to be non-magnetic and in the optimal case electrically insulating to avoid eddy currents caused by leakage fluxes, but heat-conducting for the heat discharge of the rotor losses. Naturally a compromise has to be found here.

The precise calculation of the eddy current losses is done with a 3D-FE solver with time stepping procedure for taking into account the velocity effect [6]. The results of the transient analysis were used to find suitable materials and dimensions for the carrier and housing regions.

The complete arrangement of the active parts in the rotor, shown in Fig. 12, is framed by two rings at each side made of a plastic material because in these regions the highest eddy current losses would occur when using a conducting material.

The active parts are mounted on a non-magnetic steel ring to prevent high magnetic leakage fluxes from one soft magnetic piece to the next. The electric conductivity of non-magnetic steel is relatively low and heat discharge of the rotor losses to another fixation ring made of aluminium and the aluminium housing is possible to a certain degree.

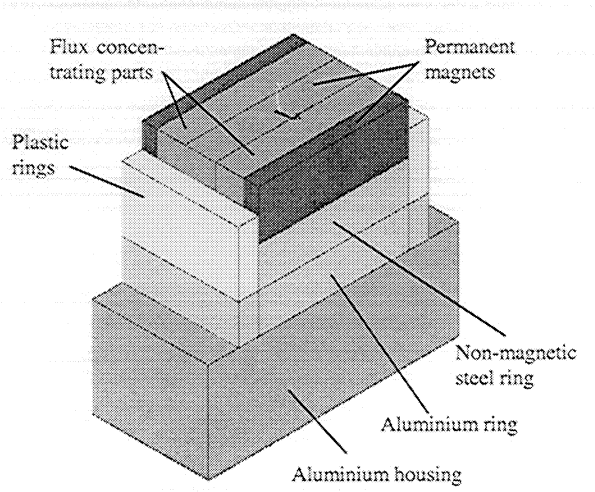

Fig. 12. Construction of the rotor

As examples for the results of the transient solution the current density distribution for the rotor position with the highest losses at 400 Hz in the permanent magnets and in the non-magnetic steel ring are shown with field plots in Fig. 13 and Fig. 14 respectively.

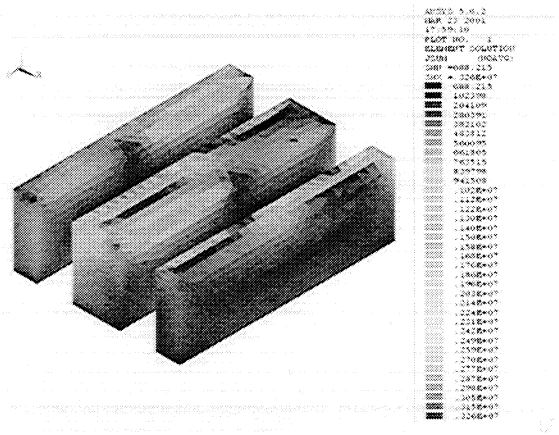

Fig. 13. Eddy current density in the permanent magnets

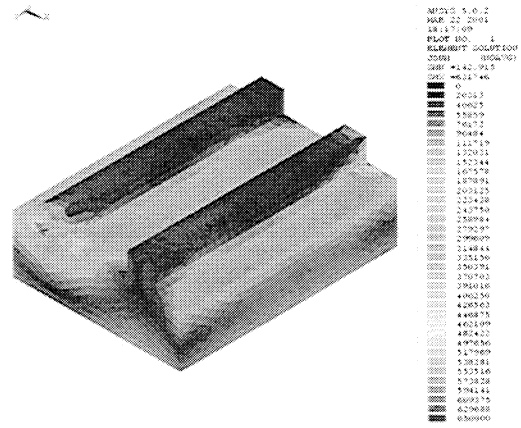

Fig. 14. Eddy current density in the non-magnetic steel ring

The critical regions in the permanent magnets are the areas near the air-gap, whereas the highest eddy currents in the non-magnetic steel ring are directly below the active parts. The teeth on the surface of the steel ring are used for mounting the flux concentrating parts with appropriate slots.
The absolute values of the eddy current losses in the carrier and housing regions are quite low in comparison with the iron and copper losses but they nevertheless lead to quite high temperatures in the rotor because of the bad cooling possibilities.

V. OPERATING RANGE OF THE MACHINE

For one phase of the transverse flux machine the equivalent circuit phasor diagram of the synchronous machine, which is shown in Fig. 15, can be used.
The possible operating range of the machine is limited by the capability of the inverter with respect to the maximum current, which restricts the output torque, and to the maximum frequency, which limits the top speed.
As it can be seen from the schematic vector diagram the inductive voltage drop is quite high and therefore the maximum inverter voltage is reached with relatively low speed.
Applying a negative direct current component (I_d) in the field weakening range reduces the phase voltage significantly and leads to extended operation limits. Besides the operating ranges the lines of constant efficiency, calculated with the approaches presented in the last section, are depicted in Fig. 16 and Fig. 17.
The negative direct current component also increases the efficiency in most of the operating points significantly, because the increased copper losses produced by the additional current component are more than compensated by the reduced iron losses.
The efficiency values given in the diagrams only represent the performance of the machine, the inverter efficiency has not been taken into account so far. This will be done in the future by dynamic simulations of the complete drive system.

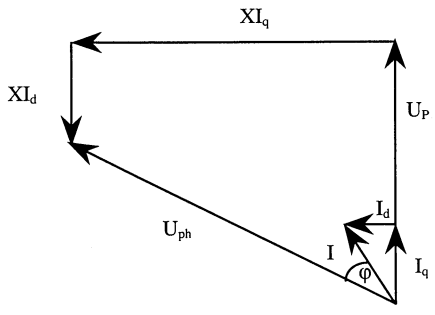

Fig. 15. Phasor diagram

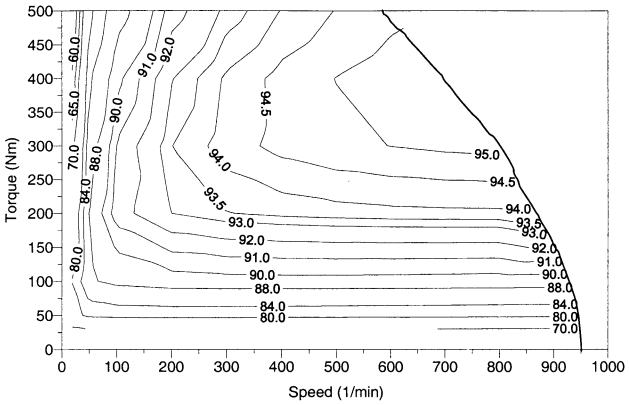

Fig. 16. Operating range with current only in quadrature axis

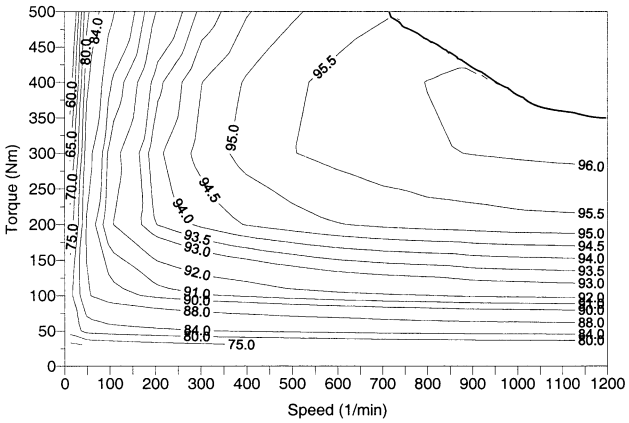

Fig. 17. Operating range with additional current in negative direct axis

VI. DATA OF THE PROTOTYPE MACHINE

Table I
Electrical data of the prototype machine

Nominal power	30.5 kW
Nominal speed	650 rpm
Nominal torque	450 Nm
Nominal phase current	73 A
Nominal phase voltage	220 V
Nominal power factor	0.62
Nominal efficiency	95 %
Nominal inductance	0.86 mH
Number of poles	40
Number of winding turns per phase	16

Table II
Dimensions and weights of the prototype machine

Air-gap diameter	295 mm
Active stator length	115 mm
Active rotor diameter	315 mm
Permanent magnet weight	3.5 kg
Copper winding weight	4 kg
Soft magnetic composite weight in the rotor	2.6 kg
Soft magnetic composite weight in the stator	19 kg
Total active weight	29 kg

VII. SUMMARY

The development of a new design of a transverse flux machine with soft magnetic composite is described in detail.
The suggested design submits an easy assembly, although the manufacturing tolerances in the active rotor parts has to be small.
The three phase variant of the transverse flux machine submits the application of standard converters. The torque per unit active mass and volume respectively reaches very high values.
The investigation of the loss mechanisms reveals the importance of suitable carrier and housing materials for minimized additional eddy current losses. A combination of plastic, non-magnetic steel and aluminium parts seems to be the most promising solution.
Especially the iron losses in the soft magnetic composite, which mainly consist of hysteresis losses, can be reduced significantly with a negative direct current component in the field weakening range.
The manufacturing of a prototype machine with the presented design is currently in progress.

VIII. REFERENCES

[1] R. Blissenbach, G. Henneberger, U. Schäfer, W. Hackmann, "Development of a transverse flux traction motor in a direct drive system", *Proc. Int. Conference on Electrical Machines (ICEM)*, Helsinki, Finland, 2000, Vol. 3 pp.1457-1460

[2] R. Blissenbach, G. Henneberger, "Numerical calculation of 3D eddy current fields in transverse flux machines with time stepping procedures", *COMPEL*, Vol. 20, No. 1, 2001, pp.152-166

[3] A.G. Jack, "Experience with the use of soft magnetic composites in electrical machines", *Proc. Int. Conference on Electrical Machines (ICEM)*, Istanbul, Turkey, 1998, Vol. 3 pp.1441-1448

[4] Ö. Krogen, P. Jansson, A.G. Jack, B.C. Mecrow, "The route from powder to an electrical machine application", *Powder Metallurgy World Congress*, Granada, Spain, 1998

[5] C.P. Maddison, B.C. Mecrow, A.G. Jack, "Claw pole geometries for high performance transverse flux machines", *Proc. Int. Conference on Electrical Machines (ICEM)*, Istanbul, Turkey, 1998, Vol. 1 pp.340-345

[6] D. Albertz, "Calculation of 3D eddy current fields using both electric and magnetic vector potential in conducting regions", *IEEE Trans. Magn.*, Vol. 34, No. 5, 1999, pp.2644-2647

[7] M. Bork, R. Blissenbach, G. Henneberger, "Identification of the loss distribution in a transverse flux machine", *Proc. Int. Conference on Electrical Machines (ICEM)*, Istanbul, Turkey, 1998, Vol. 3 pp.1826-1831